Dominici Fernando P. (Orcid ID: 0000-0002-4351-0057)

Title: Activation of angiotensin type 2 receptors prevents diabetic complications in female db/db mice by nitric oxide-mediated mechanisms

Running Title: AT_2R activation and type 2 diabetes

Fernando P. Dominici[1], Luciana C. Veiras[2], Justin Z.Y. Shen[2], Ellen A. Bernstein[2], Diego T. Quiroga[1], Ulrike M. Steckelings[3], Kenneth E. Bernstein[2,4], Jorge F. Giani[2,4]

1 Universidad de Buenos Aires, Facultad de Farmacia y Bioquímica, Departamento de Química Biológica, IQUIFIB (UBA-CONICET), Buenos Aires, Argentina.
2 Department of Biomedical Sciences, Cedars-Sinai Medical Center, Los Angeles, CA, USA.
3 IMM – Department of Cardiovascular & Renal Research, University of Southern Denmark, Odense, 5000, Denmark.
4 Department of Pathology, Cedars-Sinai Medical Center, Los Angeles, CA, USA.

Word count: 4,077 (excluding Abstract, Methods, References and Figure Legends)

Address for reprint requests and other correspondence:

Jorge F. Giani, PhD
Assistant Professor, Departments of Biomedical Sciences and Pathology
jorge.giani@cshs.org
CEDARS-SINAI MEDICAL CENTER
8700 Beverly Blvd., Davis Bldg. Room 2019: Los Angeles CA 90048
Direct 310.423.7701: cedars-sinai.edu

This article has been accepted for publication and undergone full peer review but has not been through the copyediting, typesetting, pagination and proofreading process which may lead to differences between this version and the Version of Record. Please cite this article as doi: 10.1111/bph.15241

This article is protected by copyright. All rights reserved.

Author contributions

F.P.D, U.M.S., and J.F.G. conceived and designed research; F.P.D., L.C.V., J.Z.Y.S., D.T.Q., E.A.B., and J.F.G. performed experiments; F.P.D., L.C.V., J.Z.Y.S., E.A.B., and J.F.G. interpreted results of experiments; F.P.D., L.C.V., K.E.B., and J.F.G. analyzed data; F.P.D. and J.F.G. prepared figures; F.P.D., L.C.V., J.Z.Y.S., and J.F.G. drafted manuscript; all authors revised, edited and approved the final version of manuscript.

Acknowledgements

This work was supported by National Institutes of Health Grants R01HL142672 (J.F.G.), P30DK063491 (J.F.G.), R01AI143599 (K.E.B.), P01HL129941 (K.E.B.), and T32 DK007770 (L.C.V.), American Heart Association Grants 16SDG30130015 (J.F.G.) and 17GRNT33661206 (K.E.B.), Agencia Nacional de Promoción Científica y Tecnológica of Argentina (ANPCYT) grant PICT-2014-0362 (F.P.D.) and Universidad de Buenos Aires grant UBACYT 20020130100218BA (F.P.D.)

Conflict of interests

None

Declaration of transparency and scientific rigour

This Declaration acknowledges that this paper adheres to the principles for transparent reporting and scientific rigour of preclinical research as stated in the BJP guidelines for Natural Product Research, Design and Analysis, Immunoblotting and Immunochemistry, and Animal Experimentation, and as recommended by funding agencies, publishers and other organizations engaged with supporting research.

Accepted Article

This article is protected by copyright. All rights reserved.

Abstract

Background and Purpose: The angiotensin type 2 receptor (AT_2R) plays a role in metabolism by opposing the actions triggered by the angiotensin type 1 receptor (AT_1R). Activation of AT_2R has been shown to enhance insulin sensitivity in both normal and insulin resistance animal models. In this study, we investigated the mechanism by which AT_2R activation improves metabolism in diabetic mice.

Experimental approach: Female diabetic (db/db) and non-diabetic (db/+) mice were treated for 1 month with the selective AT_2R agonist compound 21 (C21, 0.3 mg Kg^{-1} day^{-1}, subcutaneous). To evaluate whether the effects of C21 depend on nitric oxide (NO) production, a subgroup of mice were treated with C21 plus a sub-pressor dose of the NO synthase inhibitor L-NAME (0.1 mg ml^{-1}, drinking water).

Key results: C21-treated db/db mice displayed improved glucose and pyruvate tolerance compared to saline-treated db/db mice. Also, C21-treated db/db mice showed reduced liver weight and decreased hepatic lipid accumulation compared to saline-treated db/db mice. Insulin signaling analysis showed increased phosphorylation of insulin receptor, Akt and FOXO1 in the livers of C21-treated db/db mice compared to saline-treated counterparts. These findings were associated with increased adiponectin levels in plasma and adipose tissue, and reduced adipocyte size in inguinal fat. The beneficial effects of AT_2R activation were associated with increased eNOS phosphorylation, higher levels of nitric oxide metabolites, and were abolished by L-NAME.

Conclusion and implications: Chronic C21 infusion exerts beneficial metabolic effects in female diabetic db/db mice, alleviating type 2 diabetes complications, through a mechanism that involves NO production.

Accepted Article

This article is protected by copyright. All rights reserved.

Keywords: Angiotensin type 2 receptor; Akt; db/db mice; FOXO1; Gluconeogenesis; Insulin receptor; Renin-angiotensin system.

Abbreviations

Ang II, angiotensin II; AT_1R, angiotensin II type 1 receptor; AT_2R, angiotensin II type 2 receptor; C21, compound 21; FOXO1, transcription factor forkhead box O1; IR, insulin receptor; L-NAME, N(ω)-nitro-L-arginine methyl ester; NO, nitric oxide; RAS, renin angiotensin system; UCP-1, uncoupling protein 1.

Bullet point summary

What is already known:

Stimulation of the angiotensin type 2 receptor (AT_2R) has beneficial metabolic effects

What this study adds:

Administration of the C21 to female db/db mice ameliorates diabetes-induced complications including hepatic steatosis, inflammation and fibrosis and adipocyte hypertrophy. These changes were associated with increased adiponectin both in the circulation and in adipose tissue as well as improved insulin signaling in the liver. The beneficial effects of AT_2R activation were mediated through a mechanism that requires nitric oxide.

Clinical significance:

Drugs targeting the AT_2R may represent a therapeutic option to prevent diabetes and/or alleviating its complications in females.

Accepted Article

This article is protected by copyright. All rights reserved.

INTRODUCTION

Major features of type 2 diabetes associated with obesity include dysregulated glycemic profile, dyslipidemia, increased adiposity with redistribution of fat in central areas, hyperinsulinemia, increased glucose production, hyperglycemia, and hepatic steatosis (Kahn, Hull & Utzschneider, 2006). Given that the consequences of type 2 diabetes are serious and include long term severe organ and tissue damage (Papatheodorou, Banach, Bekiari, Rizzo & Edmonds, 2018), finding new therapeutic strategies to counteract this disease is essential.

The renin-angiotensin system (RAS) plays a key role in the development of metabolic syndrome and type 2 diabetes (Henriksen, 2007). Activation of the Ang II type 1 receptor (AT_1R) increases the generation of inflammatory cytokines and augments oxidative stress, that ultimately diminish the tissue sensitivity to insulin and lead to the development of insulin resistance (Forrester et al., 2018; Iimura et al., 1995). Contrarily, blockade of the AT_1R, consistently improves insulin sensitivity and glucose homeostasis in various animal models of insulin resistance and/or type 2 diabetes (Henriksen, 2007; Iimura et al., 1995; Munoz, Giani, Dominici, Turyn & Toblli, 2009; Rodriguez et al., 2018; Shiuchi et al., 2004). The role of the AT_2R in metabolic control is less known, but, recent evidence suggests that pharmacological activation of the AT_2R blocks the production of inflammatory cytokines, and lowers oxidative stress, thereby improving insulin sensitivity and secretion (Carey, 2017; Santos, Oudit, Verano-Braga, Canta, Steckelings & Bader, 2019). Although AT_1R antagonists and ACE inhibitors are administered for the purpose of alleviating diabetes complications such as diabetic nephropathy and vascular disease in humans (Umanath & Lewis, 2018), novel formulations that modulate the AT_2R may represent a therapeutic breakthrough (Paulis, Foulquier, Namsolleck, Recarti, Steckelings & Unger, 2016). In this sense, the discovery and characterization of the selective small-molecule agonist, compound 21 (C21), has been a major advance in the field (Paulis, Foulquier, Namsolleck, Recarti, Steckelings & Unger, 2016; Santos, Oudit, Verano-Braga, Canta, Steckelings & Bader, 2019; Steckelings et al., 2011). Administration of C21 exerts a beneficial effect on insulin sensitivity in both diabetic and insulin resistant animal models (Ohshima et al., 2012; Shao, Yu & Gao, 2014; Shao, Zucker & Gao, 2013; Than, Xu, Li, Leow, Sun & Chen, 2017; Wang, Wang, Li & Leung, 2017). In addition, administration of C21 enhances insulin delivery and metabolic action in rat skeletal muscle (Yan et al., 2018). Together with our recent observation that prolonged C21 administration enhances insulin sensitivity in mice (Quiroga et al., 2018), these findings support the potential role of AT_2R as a modulator of insulin action and glucose homeostasis.

This article is protected by copyright. All rights reserved.

To further characterize the therapeutic effect of AT_2R activation in metabolic-related diseases, we studied the effect of C21 on db/db mice, a mouse model of type 2 diabetes and obesity-induced hyperglycemia. To gain insight into the potential participation of nitric oxide (NO) in the beneficial effects of C21, a group of diabetic mice was treated concomitantly with a sub-pressor dose of the NO synthase inhibitor Nω-Nitro-L-arginine methyl ester hydrochloride (L-NAME). In general, studies on mouse models of type 2 diabetes have historically employed male mice (Mauvais-Jarvis, 2015). However, preclinical studies have demonstrated that the beneficial AT_2R-mediated effects on cardiovascular and renal function are enhanced in females, primarily in rodent models (Hilliard et al., 2014; Hilliard, Jones, Steckelings, Unger, Widdop & Denton, 2012; Silva-Antonialli et al., 2004). The main hypothesis behind the current work is that C21 treatment ameliorates type 2 diabetes-associated complications through a NO-mediated mechanism. To that end, we analyzed glucose and pyruvate tolerance, circulating and tissue TNF-α, changes in hepatic steatosis and fibrosis and circulating and adipose tissue content of both adiponectin and resistin in db/db female mice that were treated for a month with C21 in absence or presence of L-NAME. To gain further insight into the mechanism behind the beneficial effects of C21, we analyzed the status of the insulin signaling system (insulin receptor, Akt and FOXO1) as well as the phosphorylation and protein levels of eNOS in both liver and adipose tissue of the experimental animals.

Accepted Article

This article is protected by copyright. All rights reserved.

METHODS

Mice and Study Design

All animal procedures were approved by the Cedars-Sinai Institutional Animal Care and Use Committee and conducted in accordance with the NIH Guide for the Care and Use of Laboratory Animals. The animals were treated humanely, and all efforts were made to minimize the animals' suffering and the number of mice used in the study. All results are reported in compliance with the ARRIVE guidelines (Kilkenny, Browne, Cuthill, Emerson & Altman, 2010). Animals were maintained under controlled light and temperature conditions and had free access to water and standard chow diet. Experiments were performed on 16-week-old db/db female mice (B6.BKS(D)-Lepr^{db}/J, stock #697) [IMSR_JAX:000697] and their respective db/+ (heterozygous) controls purchased from Jackson Laboratories (Bar Harbor, ME, USA).

The group size of all animal experiment was designed to at least n = 5. Taking into consideration the expected attrition owing to long-term treatment, we increased the group size of mice to n = 7. All group size was estimated by power analysis (Schmidt, Lo & Hollestein, 2018). To evaluate the effects of chronic AT_2R agonism, mice (n=7 per group) received a 4-week subcutaneous treatment with either sterile saline (vehicle controls) or C21 (0.3 mg kg^{-1} day^{-1}, Vicore Pharma AB, Göteborg, Sweden) using osmotic minipumps (Alzet, Catalog #1004, Cupertino, CA). We generated groups of equal size using a completely randomized design in the experiment. The experiments were blind to the operators and analyzers. The dose of C21 was selected based on previous published protocols (Nag, Khan, Samuel, Ali & Hussain, 2015). To test the role of NO, a subgroup of mice (n=7) received C21 plus a sub-pressor dose of L-NAME (0.1 mg ml^{-1}, Bachem, Torrance, CA, USA) in drinking water. Systolic blood pressure (SBP) was measured weekly in conscious mice using the tail-cuff method (Visitech BP2000 System, Visitech Systems Inc.; Apex, NC, USA) after proper training. SBP was measured 25 times for each time point. At day 24, mice were fasted for 6 hours and a glucose tolerance test (GTT) was conducted as described below. After a 2-day resting period (day 26), mice were fasted again for 6 hours to perform a pyruvate tolerance test (PTT) as detailed below. At day 28, mice were euthanized via conscious decapitation after a 6-hour fast. Liver, heart, and inguinal and perirenal adipose tissues were harvested and used for histological analysis, cytokine assessment, and the study of key insulin signaling-related proteins by western blotting as described in sections below.

Urine Collection and Albuminuria

This article is protected by copyright. All rights reserved.

For urine collection, mice were placed in metabolic cages (Tecniplast, Verese, VA, USA) for 6 hours with free access to water and standard chow diet (Bio Serv; Flemington, NJ, USA). Urine was collected in refrigerated tubes, centrifuged at 2,000x*g* for 10 minutes at 4°C and aliquoted for further analysis. Urine albumin levels were measured using an ELISA commercial kit (Albuwell, Exocell, Philadelphia, PA, USA). Systemic NO synthase inhibition by L-NAME was confirmed by measuring urinary excretion of NO metabolites (NOx) using the Griess assay (Promega Corp., Fitchburg, WI, USA). Creatinine levels were assessed using the Creatinine LiquiColor Test (EKF Diagnostics Inc, Boeme, TX, USA) as previously described (Eriguchi et al., 2018). Both urine albumin and NOx excretion values were corrected by urine creatinine levels.

Glucose and Pyruvate Tolerance Test

Mice were fasted for 6 hours prior to commencement of a glucose tolerance test (GTT). Baseline glucose levels were sampled from tail blood using a Contour Blood Glucose Monitoring System (Bayer HealthCare LLC; Tarrytown, NY, USA). Then, mice were injected I.P. with 2 grams of glucose per kilogram of body weight using a 25% w/v solution prepared in sterile phosphate buffer saline (PBS). Blood glucose level was measured at 15, 30, 60, and 120 min post-injection. After 2 days, a pyruvate tolerance test (PTT) was performed. For this, mice were fasted for 6 hours and then injected I.P. with 1 gram of pyruvate per kg of body weight using a 10% w/v solution prepared in sterile PBS. Blood glucose levels were then measured at 15, 30, 60, and 120 min post-injection via tail-end bleed.

Insulin, adiponectin, and resistin assessment in plasma

Mice were euthanized by conscious decapitation, blood was collected in EDTA-coated tubes, centrifuged at 2,000x*g* for 10 minutes at 4°C and plasma was stored at -80°C until analysis. Plasma insulin was measured using the Ultra-Sensitive Mouse Insulin ELISA Kit (Crystal Chem, Elk Grove Village, IL, USA), plasma adiponectin was measured using the Mouse Adiponectin ELISA Kit (Crystal Chem), and plasma resistin was measured using a Mouse Resistin ELISA kit (RayBiotech, Peachtree Corners, GA, USA) following the manufacturer's instructions.

Tissue homogenization and ELISA

Perirenal and inguinal adipose tissue (200 mg) were homogenized in 500 µl of Mammalian Protein Extraction Reagent (M-PER buffer, Thermo Scientific; Waltham, MA, USA)

This article is protected by copyright. All rights reserved.

containing 0.5 mM disodium EDTA, 0.2 mM phenylmethylsulfonyl fluoride, 9 μg ml^{-1} aprotinin, 5 μg ml^{-1} of phosphatase inhibitor cocktail 3 (P2850, Sigma-Aldrich, St. Louis, MO, USA). Each sample was homogenized for 5 min at a medium-speed setting with an Ultra-Turrax T25 (IKA Labortechnik, Wilmington, NC, USA) and placed on ice for 30 min. Samples were then centrifuged at 20,000 x*g* for 10 minutes at 4°C, the lipid layer was removed, and protein concentrations were determined using a bicinchoninic acid protein assay (BCA assay. Pierce Thermo Scientific, Rockford, IL, USA). For liver, 100 mg of tissue were homogenized in 500 ul of radioimmunoprecipitation assay buffer (RIPA Pierce, Thermo Scientific; Waltham, MA, USA) containing 0.5 mM disodium EDTA, 0.2 mM PMSF, 9 μg ml^{-1} aprotinin, 5 μg ml^{-1} of a phosphatase inhibitor cocktail (P2850, Sigma-Aldrich). After centrifugation at 20,000 x*g* for 10 minutes at 4°C, the supernatant was collected, and the protein concentration was determined using the BCA assay. The levels of IL-1β and TNF-α were measured in whole-tissue homogenates using commercially available ELISA kits (eBioscience, San Diego, CA, USA).

Real-time PCR

To quantify the gene expression of the AT_2R in liver, total RNA was isolated from liver samples using RNeasy Mini-Kit (Qiagen, Valencia, CA, USA) following the manufacturer's instructions. Synthesis of complementary DNA (cDNA) was performed using 1 μg of total RNA and Maxima™ H Minus cDNA Synthesis Master Mix (ThermoFisher, Rockford, IL, USA). Real-time PCR was performed in a 10-μl reaction mixture consisting of 5 μl iTaq Universal SYBR Green Supermix (Bio-Rad, Hercules, CA, USA), 1 μl cDNA and 0.3 μM of primers for each specific target. Amplification was performed at 95°C for 15 min, followed by 45 cycles at 95°C for 20 s and 60°C for 60 s. The relative amount of the target mRNA was normalized with the housekeeping gene GAPDH. The primers were as follows: AT2R 5'-GGGTAAACAGACCCAGCAAA-3' and 5'-CTGGAACTGTGCCCAGAAAT-3', GAPDH 5'-AACTTTGGCATTGTGGAAGG-3' and 5'-GGATGCAGGGATGATGTTCT-3'.

Western Blotting

Western blotting procedures used in this study comply with the recommendations made by the *British Journal of Pharmacology* (Alexander et al., 2018). Liver and adipose tissue extracts were denatured, resolved by SDS-PAGE, transferred into PVDF membranes (Millipore Immobilon-FL; EMD Millipore, Billerica, MA), and finally probed with specific antibodies for adiponectin/Acrp30 [AB_2221787] (R&D Systems; Minneapolis, MN), uncoupling protein 1

This article is protected by copyright. All rights reserved.

[AB_2241459] (UCP-1, ThermoFisher, Rockford, IL), IR β subunit [AB_1950593] (GeneTex, Irvine, CA) and phospho-Tyr 1158/1162/1163 insulin receptor β subunit [AB_568831] (Millipore, Burlington, MA), Akt [AB_915783] and phospho-Ser 473 Akt [AB_2315049] (Cell Signaling, Danvers, MA), and FOXO1 [AB_823503] and phospho-Ser 256 FOXO1 [AB_329831] (Cell Signaling). Signals were detected with the Odyssey Infrared Imaging System (LI-COR, Lincoln, NE, USA) and quantified by accompanying software. Test values were normalized to control group values for unwanted sources of variation. To assess the error of the control group, each individual control value was divided by average intensity obtained for the control group (db/+ mice). The intensity value of each individual band was divided by the average intensity obtained for the control group (db/+ mice). The units shown in bar graphs were obtained by considering the average value of intensity of each specific band in the control group as 100% and transforming them to 1 arbitrary unit ± S.D.).

For protein loading control and normalization, membranes were re-probed with antibodies against β-actin [AB_476697] for liver or GAPDH [AB_796208] (Sigma-Aldrich) for adipose tissue. The level of each protein evaluated was normalized to the level of β-actin or GAPDH from control samples to avoid sources of variation. The molecular weight of proteins was estimated using prestained protein markers (Bio-Rad, Hercules, CA). **Supplemental table 1** catalogs the amounts assayed, antibodies, vendors, and dilutions used.

Masson's Trichrome and ORO Staining

For the assessment of interstitial hepatic fibrosis, liver samples were fixed with 10% buffered formalin and embedded in paraffin. Four-μm-thick sections were deparaffinized, rehydrated, and stained with Masson's trichrome. The analysis of lipid droplets in the liver was performed using the oil red O (ORO) staining (Mehlem, Hagberg, Muhl, Eriksson & Falkevall, 2013). For this, immediately after collection, liver samples were snap-frozen in liquid nitrogen and stored at -80^{o}C. Later, tissues were embedded in Tissue-Tek, and 8-μm-thick sections were cut and air-dried. Then sections were fixed in formalin for 15 min, washed for 2 min with tap water, and rinsed with 60% isopropanol for 2 min. To make the ORO working solution, 30 ml of ORO stock solution (Sigma-Aldrich, Cat#: O1391) were diluted with 20 ml of distilled water and protected from light. Fixed sections were then stained with the working solution horizontally for 15 min and rinsed 3 times with 60% isopropanol (1 min each). Samples were counterstained with hematoxylin for 1 min and immediately evaluated. Images were acquired using an RVL-100-G Microscope (Echo Laboratories, San Diego, CA, USA) at 20x magnification.

This article is protected by copyright. All rights reserved.

Morphological Analysis of Adipose Tissue

Perirenal and inguinal adipose tissue samples were preserved in 10% formalin solution and embedded in paraffin. Three-µm-thick paraffin-embedded sections were then deparaffinized in xylene and rehydrated to water through ethanol at 100°, 96°, and 80°C and stained with H&E (Quiroga et al., 2018). For each individual sample, adipocyte size was measured in five microscopic fields in single-blinded condition and expressed in μm^2. The size of 60 adipocytes was determined for each mouse. Images were acquired as described above.

Data and analysis

The data and statistical analysis comply with the recommendations and requirements of the *British Journal of Pharmacology* (Curtis et al., 2018). Animals were randomly distributed between groups. All statistical analyses were performed using GraphPad Prism 8 (GraphPad Software, San Diego, CA) [SCR_002798]. The threshold for statistical significance was set at the level of P being 0.05. Therefore, in all cases, $P<0.05$ was considered statistically significant. Statistical analysis was undertaken only for studies where each group size was at least n=5. No additional data, involving group sizes of $n < 5$ was used or analyzed. Every individual value obtained was included in the analysis, no outliers were detected. Data are presented as individual dot plots and the mean ± SD. Differences among experimental groups were compared by two-way ANOVA. Tukey's post hoc tests were performed only if the F value in ANOVA achieved the required level of statistical significance ($P<0.05$), and there was no significant variance in homogeneity. The declared group size is the number of independent values. Statistical analysis was done using these independent values.

Nomenclature of Targets and Ligands

Key protein targets and ligands in this article are hyperlinked to corresponding entries in http://www.guidetopharmacology.org, the common portal for data from the IUPHAR/BPS Guide to PHARMACOLOGY (Harding et al., 2018), and are permanently archived in the Concise Guide to PHARMACOLOGY 2019/20: Chapter S21 G protein-coupled receptors (Alexander et al., 2019).

This article is protected by copyright. All rights reserved.

RESULTS

C21 treatment and metabolic parameters

Female diabetic (db/db) mice and their corresponding non-diabetic (db/+) littermates received subcutaneous C21 or saline for 1 month via osmotic mini pumps. Another subgroup of mice was simultaneously treated with C21 and a sub-pressor dose of L-NAME in drinking water. Initially, we confirmed that L-NAME inhibited systemic nitric oxide synthase without affecting blood pressure. Compound 21 induced an increase in urinary nitric oxide metabolites (NOx: nitrites and nitrates) in db/db mice compared to db/db mice receiving saline (~2-fold, Supplemental Figure 1A). Although this increase was completely prevented with L-NAME, no significant changes in blood pressure were observed (Supplemental Figure 1A,B). In both db/db and db/+ mice treated with C21+L-NAME, systolic blood pressure remained unchanged during the whole experiment (Supplemental Figure 1B). The absence of significant albuminuria (Supplemental Figure 1C) and cardiac hypertrophy (Table 1) in L-NAME-treated mice adds further evidence that no changes in blood pressure occurred during the treatment.

As expected, body weight and blood glucose were significantly increased in db/db compared to non-diabetic db/+ mice at the beginning of the experiment (Supplemental Figure 2). Treatment with C21 or C21+L-NAME did not modify these parameters (Figure 1A-B). Plasma insulin and the Homeostatic Model Assessment of Insulin Resistance (HOMA-IR) index were also significantly increased in db/db compared to non-diabetic controls (Figure 1C-D). Interestingly, treatment of db/db mice with C21 induced a significant reduction (39%) of the HOMA-IR that was reverted by the concomitant administration of L-NAME (Figure 1C-D). Interestingly, C21 induced a significant increase of plasma adiponectin in db/db mice (~2.3-fold, Figure 1E) that was blunted in the presence of L-NAME (Figure 1E). Plasma resistin levels were similar among all experimental groups (Figure 1F).

To gain further insight into the metabolic profile of db/db mice and the effect of C21, a glucose tolerance test (GTT) and a pyruvate tolerance test (PTT) were performed at the end of the experiment. Diabetic db/db mice displayed a significant intolerance to an acute glucose load compared to non-diabetic db/+ littermates. This observation was true for non-treated db/db and db/db mice receiving either C21 or C21+L-NAME (Figure 2A). However, when comparing the area under the curve (AUC), C21-treated db/db mice showed a significant AUC reduction (from 4178 ± 216 to 3544 ± 304 mg dl^{-1} min^{-1}, Figure 2B,) compared to non-treated db/db mice. Similarly, a pyruvate tolerance test to evaluate liver gluconeogenesis revealed that, compared to db/+ mice, db/db mice have an exaggerated blood glucose elevation in response to pyruvate (Figure 2C). Again, this response was also improved after C21 treatment (from

This article is protected by copyright. All rights reserved.

4059 ± 202 to 3296 ± 217 mg dl^{-1} min^{-1}, Figure 2D). The concomitant administration of C21 plus L-NAME blunted the beneficial effect of C21 on both glucose (Figure 2B) and pyruvate handling (Figure 2D).

Effects of C21 on inguinal and perirenal adipose tissue

Both inguinal and perirenal adipose tissue weight were increased in db/db mice compared to db/+ mice. Inguinal fat showed a ~4.5-fold increase while perirenal fat displayed a ~5.2-fold increase in untreated db/db mice compared to db/+ mice (Table 1). In C21-treated db/db mice, inguinal adipose tissue weight was significantly reduced compared to non-treated db/db mice (from 1.8 ± 0.5 to 1.2 ± 0.5 mg, Table 1). Perirenal fat weight of db/db mice was also lower in the C21-treated animals (2.6 ± 0.6 in untreated db/db mice vs. 1.8 ± 0.4 mg in C21-treated animals, Table 1). In db/db mice treated with C21+L-NAME, both the inguinal and perirenal adipose tissue weight was indistinguishable from untreated db/db mice suggesting that the effect of C21 was counteracted by L-NAME (Table 1).

Further histological analysis of inguinal adipose tissue revealed that db/db mice receiving saline showed a significant increase in adipocyte size compared to non-diabetic controls. Although C21-treated db/db mice still displayed larger adipocytes compared to non-diabetic mice, their size was significantly reduced compared to non-treated db/db mice (8346 ± 1519 vs. 5617 ± 1186 μm^2, Figure 3A-B). Even more important, adiponectin levels were significantly increased by C21 in inguinal adipose tissue from db/db mice (~2.4-fold increase, Figure 3C). UCP-1, a marker of adipose tissue browning, was significantly reduced in db/db mice compared to db/+ controls. Although C21 induced a slight increase of UCP-1 adipose tissue content in db/db mice, this change did not reach statistical significance (Figure 3D). As observed for other parameters, blockade of NO production with L-NAME blunted the effects of C21 regarding adipocyte size and tissue adiponectin content (Figure 3A-C). Contrarily, perirenal adipose tissue from db/db mice appeared less responsive to C21 as none of the parameters evaluated were modified in this fat depot after a 4-week administration of C21 or C21+L-NAME (Supplemental Figure 3).

Effects of C21 on hepatic steatosis and fibrosis

To evaluate whether the beneficial effects of C21 were also observed in liver, we evaluated hepatic lipid deposition and fibrosis at the end of the experiment. Diabetic db/db mice displayed an increased liver weight compared to their db/+ counterparts. However, C21-treated db/db mice showed a significant reduction in liver weight compared to non-treated db/db mice (2.7

This article is protected by copyright. All rights reserved.

± 0.8 vs. 3.7 ± 0.7 g, Table 1). C21 also decreased hepatic lipid deposition in db/db mice. Histological analysis of liver sections stained with oil red O showed that C21-treated db/db mice had less lipid deposition (~48% reduction, Figure 4A-B) and smaller lipid droplets (~60% reduction, Figure 4C) compared to non-treated db/db mice. Finally, histological evaluation of liver fibrosis by Masson's trichrome staining revealed a significant increase in extracellular matrix deposition in the liver of untreated db/db mice, with a significant reduction in the C21-treated db/db mice (~50%, Figure 4D-E). Although nitric oxide inhibition with L-NAME did not modify the effect of C21 on liver weight (Table 1), it abolished the protective effect of C21 on hepatic lipid deposition. Diabetic mice receiving both C21 and L-NAME showed increased lipid deposition (Figure 4B) and larger lipid droplets (Figure 4C) in the liver compared to C21-treated db/db mice.

Role of C21 on hepatic insulin signaling of female db/db mice

To get a deeper insight into the molecular mechanism that mediates the beneficial effects of C21 on metabolism, we evaluated the phosphorylation and total abundance of IR, Akt and FOXO1, key intracellular molecules associated with the insulin signaling pathway in the liver. In non-treated db/db mice, despite very high plasma insulin levels, the phosphorylation of IR was negligible and not different from db/+ mice (Figure 5A). However, in C21-treated db/db mice, basal IR phosphorylation was significantly higher compared to non-treated db/db mice (3.5 ± 1.5 vs. 1.5 ± 0.4 arbitrary units). The greater hepatic IR activation displayed by C21-treated db/db mice was blunted by concomitant administration of L-NAME (Figure 5A). Akt phosphorylation showed no changes between non-treated db/db and db/+ mice. However, db/db mice treated with C21 displayed an increased Akt phosphorylation compared to non-treated db/db mice (2.6 ± 0.9 vs. 1.6 ± 0.4 arbitrary units, Figure 5B). In accordance to IR phosphorylation, L-NAME reduced Akt phosphorylation in db/db mice to levels that were similar to those found at baseline (Figure 5B). No significant changes were observed in total protein expression of either IR or Akt (Figure 5A-B). Hepatic FOXO1 phosphorylation, a major regulator of hepatic gluconeogenesis, was increased in db/db mice compared to db/+ littermates. However, C21-treated db/db mice displayed significantly higher FOXO1 phosphorylation compared to non-treated db/db (Figure 5C). As shown for the other signaling molecules analyzed, the effect of C21 was blunted in the presence of a sub-pressor dose of L-NAME (Figure 5C). When compared to their respective db/+ group, db/db mice displayed a decreased expression of total FOXO1 in the liver that was not modified by C21 treatment

This article is protected by copyright. All rights reserved.

(Figure 5C). Finally, the FOXO1 phosphorylation-to-total protein ratio was higher in db/db mice treated with C21 compared to non-treated db/db mice (Figure 5C).

C21 decreases TNF-α abundance in liver.

To determine whether the beneficial effects of C21 were associated with the inhibition of inflammation, we evaluated the hepatic and adipose tissue content of TNF-α and IL-1β, two proinflammatory cytokines widely associated with metabolic abnormalities during obesity and diabetes. Hepatic TNF-α abundance was significantly increased in db/db mice compared to non-diabetic controls (161 ± 17 vs. 55 ± 17 pg/mg of protein, Figure 6A). Interestingly, db/db mice receiving C21 for 1 month showed a significant reduction of TNF-α compared to non-treated db/db mice (83 ± 37 vs 161 ± 28 pg/mg of protein, Figure 6A). In line with previous findings, co-administration of C21 with L-NAME blunted this protective response indicating a role of NO in the C21-mediated anti-inflammatory effect (Figure 6A). IL-1β was also increased in the liver of db/db mice compared to db/+ mice (54 ± 9 vs. 15 ± 5 pg/mg of protein, Figure 6B). Notably, this inflammatory cytokine was significantly reduced by C21 treatment (from 54 ± 9 to 35 ± 14 pg/mg liver). Again, C21+L-NAME treatment blunted this reduction (Figure 6B). Similar studies were performed in inguinal and perirenal adipose tissue. In those adipose tissue depots, both TNF-α and IL-1β were significantly elevated in all db/db experimental groups compared to non-diabetic db/+ mice (Figures 6C-F) and remained unchanged after C21 treatment. These data indicate that, at least in this experimental model of type 2 diabetes, the anti-inflammatory effect of C21 is primarily observed in the liver. The analysis of hepatic AT_2R expression by RT-PCR adds further evidence supporting a role of C21 in the liver of female diabetic mice. As shown in Supplemental Figure 4, db/db mice have, although not significant, higher expression of AT_2R in the liver compared to db/+ control littermates. This increase was similar in all db/db experimental groups (Supplemental Figure 4).

C21 increases the phosphorylation of eNOS in the liver and inguinal adipose tissue of female db/db mice.

Further evidence supporting the role of NO in C21 beneficial effects was obtained from the assessment of total abundance and phosphorylation of eNOS at Ser1177 in liver and inguinal adipose tissue by Western blot. In the liver of non-treated mice, the level of eNOS phosphorylation was similar between db/+ and db/db mice. However, in inguinal adipose tissue, db/db displayed significantly lower phosphorylated eNOS compared to the non-treated

This article is protected by copyright. All rights reserved.

db/+ mice (1.0 ± 0.3 vs. 0.4 ± 0.2 arbitrary units). In db/+ mice, C21 increased phosphorylated eNOS levels in the liver (from 1.0 ± 0.2 to 2.4 ± 0.8 arbitrary units, Figure 7A) but not in inguinal fat (Figure 7B). However, in db/db mice, C21 significantly increased the phosphorylation of eNOS in both liver (from 1.2 ± 0.3 to 4.0 ± 1.1 arbitrary units, Figure 7A) and inguinal fat (0.4 ± 0.2 to 1.3 ± 0.3 arbitrary units, Figure 7B). In both db/+ and db/db mice, L-NAME blunted C21-induced eNOS phosphorylation. Mice treated with C21 plus L-NAME displayed eNOS phosphorylation levels that were indistinguishable from non-treated mice (Figure 7A-B). In liver, both db/+ and db/db mice displayed similar levels of total eNOS (Figure 7A). In inguinal adipose tissue, the levels of eNOS were significantly decreased in db/db compared to db/+ (Figure 7B). Neither C21 nor L-NAME modified the total abundance of eNOS in these tissues (Figure 7-B). Further analysis revealed that C21 increased the phosphorylation-to-protein ratio of eNOS in both liver and inguinal adipose tissue of db/db mice. This increase was prevented by L-NAME chronic administration (Figure 7A-B).

Accepted Article

This article is protected by copyright. All rights reserved.

DISCUSSION

The main findings of our current study were as follows: 1) treatment with C21 improved glucose and pyruvate tolerance in db/db mice, 2) C21-treated db/db mice showed reduced liver weight, decreased hepatic levels of TNF-α, IL-1β, lipid accumulation and lower liver fibrosis compared to db/db mice receiving vehicle, 3) these changes were associated with a significant improvement of insulin signaling (increased IR, Akt and FOXO1 phosphorylation) in the livers of diabetic animals, 4) chronic AT_2R agonism led to increased levels of adiponectin both in the circulation and in inguinal adipose tissue as well as reduced adipocyte size in inguinal fat, 5) C21 increased the phosphorylation of eNOS at Ser1177 in liver and inguinal adipose tissue, and 6) most of the beneficial effects resulting from AT_2R stimulation through C21 administration were significantly prevented by the concomitant administration of L-NAME, and indicating a major participation for NO in these positive effects.

Previous studies in animal models of metabolic disorders indicated beneficial effects of AT_2R stimulation using C21 *in vivo.* Namely, reduction of body weight and fat mass and improvement of insulin sensitivity in type 2 diabetic KKAy mice (Ohshima et al., 2012) and in high-fructose/high-fat fed rats (Shum et al., 2013). Interestingly, C21 also improved glucose tolerance and insulin sensitivity in mice fed a regular diet (Quiroga et al., 2018). The db/db mouse is extreme in having a marked increase in body weight, fat mass, hyperglycemia and pronounced hyperinsulinemia. Thus, the improvement in glucose tolerance and pyruvate tolerance (an indication of hepatic gluconeogenesis) after C21 treatment is both novel and marked. Aside from the IR, Akt signaling is central to hepatocellular insulin action and coordinates all insulin effects in the liver including the gluconeogenic capacity (Petersen & Shulman, 2018). The transcription factor FOXO1 stimulates a gluconeogenic transcriptional program and is repressed after phosphorylation by Akt (Petersen & Shulman, 2018). Interestingly, although protein levels of FOXO1 were not modified by C21 treatment, this therapy led to an increase in FOXO1 phosphorylation, indicating further repression of gluconeogenesis. Thus, we postulate that the beneficial metabolic effects of C21 treatment in db/db mice could be ascribed to the concomitant increased phosphorylation of major hepatic insulin signaling components. This observation is novel and adds to the knowledge of the mechanisms by which AT_2R stimulation improves insulin action.

One of the major findings of the current study is the identification of favorable effects of C21 on liver steatosis and fibrosis. Many lines of evidence have indicated that obesity is closely linked to a chronic inflammatory state, which contributes to metabolic disorders (Shoelson,

This article is protected by copyright. All rights reserved.

Lee & Goldfine, 2006). Among these complications, non-alcoholic steatohepatitis (NASH), a progressive liver disease characterized by hepatic steatosis that leads to inflammation, fibrosis, and cirrhosis stands out (Tilg & Moschen, 2010). Currently, there is no treatment for this disease, that is thought to begin with excessive fat accumulation in the liver, followed by aggravating factors such as oxidative stress, inflammatory cytokines, and endotoxins (Tilg & Moschen, 2010). In preclinical studies, Ang II has been associated with the development of NASH since blockade of AT_1Rs has been reported to ameliorate this condition (Ran, Hirano & Adachi, 2004). The AT_1R, which is localized in hepatocytes, bile duct cells, hepatic stellate cells (HSCs), myofibroblasts, Kupffer cells and vascular endothelial cells, mediates most of the actions of Ang II in the liver (Warner, Lubel, McCaughan & Angus, 2007). However, some studies also reported AT_2R gene expression in liver tissue (Bataller et al., 2003; Nabeshima et al., 2006). Interestingly, we observed that AT_2R is slightly increased in db/db mice compared to non-diabetic littermates. This suggests that our current results showing decreased fat accumulation and anti-fibrogenic effects associated with AT_2R activation are likely due to direct activation of liver AT_2Rs in diabetic mice. TNF-α is a key player involved in the establishment of liver fibrosis. This cytokine, mainly released by hepatocytes or Kupffer cells, activates hepatic stellate cells in a paracrine manner and mediates chronic liver injury and inflammation (Yang & Seki, 2015). Our current results showing decreased hepatic fibrosis after treatment with C21 correlates well with the decreased hepatic TNF-α and IL-1β levels observed in C21-treated diabetic mice. Previous studies showed that AT_1R blockade suppresses the recruitment of macrophages to the liver and decreases TNF-α expression (Toblli, Munoz, Cao, Mella, Pereyra & Mastai, 2008). In view of our current data, the amelioration of NASH observed after AT_1R antagonism could be ascribed, at least in part, to the interaction of Ang II with liver AT_2Rs.

In humans, adipose cell enlargement in association with decreased expression of lipogenic genes and expansion of visceral adipose tissue are mediators of obesity-related insulin resistance (McLaughlin et al., 2016; Salans, Knittle & Hirsch, 1968). Chronic treatment with C21 has been shown to reduce the size of hypertrophic adipocytes and adipose tissue mass in high-fat diet fed rats (Nag, Khan, Samuel, Ali & Hussain, 2015; Shum et al., 2013). Also, we have previously reported that a decreased number of large adipocytes and increased number of new, small adipocytes after treatment of C57BL/6 mice with C21 (Quiroga et al., 2018). Our current results in db/db mice showing decreased inguinal fat and reduced adipocyte size after

This article is protected by copyright. All rights reserved.

treatment with the AT_2R agonist, highlight the potential therapeutic activity of AT_2R activation in the treatment of obesity-associated disorders.

Adiponectin is a hormone secreted by white adipose tissue with insulin-sensitizing properties. Thus, reduction in the levels of this adipokine are associated with the development of metabolic syndrome and type 2 diabetes (Fang & Sweeney, 2006). In mice, administration of adiponectin lowers glycemia and improves insulin action (Berg, Combs, Du, Brownlee & Scherer, 2001; Kubota et al., 2002). Thus, the increase in adiponectin levels detected after treatment with C21 might contribute to the improvement of glucose and pyruvate tolerance. In line with current findings, treatment with C21 has been reported to increase serum adiponectin levels both in diet-induced insulin-resistant rats (Shum et al., 2013) and in normal mice (Quiroga et al., 2018; Than, Xu, Li, Leow, Sun & Chen, 2017). Collectively, previous reports and current findings suggest that increased tissue and circulating adiponectin levels could be considered a readout of *in vivo* AT_2R activation. We and others have previously analyzed the effects of AT_2R activation on the levels of UCP-1 in adipose tissue and found an increase in this marker of browning as indicative of improved thermogenesis (Quiroga et al., 2018; Than, Xu, Li, Leow, Sun & Chen, 2017). Similar results were recently reported in mice fed a high-fat diet (Nag, Patel, Mani & Hussain, 2019). In contrast to these findings, UCP-1 levels in adipose tissue were not altered by C21 treatment neither in db/+ nor in db/db mice. Differences in the animal model, dose, time and route of administration could explain this result. Also, a limitation of the current study is that males were not employed to draw a broader conclusion on the beneficial effects of C21 in db/db mice.

One of the most important findings of the present study is that NO mediates most of the beneficial actions of C21 in type 2 diabetes-related complications. Although the knowledge of the physiological roles of the AT_2R has increased significantly, the information regarding the signaling pathways triggered by AT_2R activation is scarce. Activation of AT_2R is known to be associated with stimulation of NO production (Siragy & Carey, 1997; Steckelings, Kaschina & Unger, 2005; Takata et al., 2015). In this area, the spectrum of AT_2R signaling has recently been expanded with the report showing the participation of the Ser/Thr kinase Akt in AT_2R-mediated NO production (Peluso et al., 2018). Also, a recently published study shows that AT_2R activation inhibits fatty acid uptake in adipocytes through a NO-mediated mechanism (Nag, Patel, Mani & Hussain, 2019). However, the exact contribution of NO to the beneficial effects of C21 *in vivo* was not yet addressed. Several studies have underscored NO to have both anti-obesogenic and insulin-sensitizing properties (Sansbury & Hill, 2014). NO increases fat oxidation in peripheral tissues and decreases lipid synthesis in liver. It also increases transport

This article is protected by copyright. All rights reserved.

of insulin and glucose to key peripheral tissues and regulates gluconeogenesis (Sansbury & Hill, 2014). Our studies demonstrate that chronic C21 administration increased the phosphorylation of eNOS at Ser1177 in liver and inguinal adipose tissue of db/db mice. This was associated with increased urinary NOx. Both eNOS phosphorylation and urinary NOx were reduced in db/db mice receiving a sub-pressor dose of L-NAME. Thus, preventing C21-induced NO synthesis blunted many of the beneficial effects of C21 during diabetes. In non-diabetic mice, C21 did not modify NOx and it only increased eNOS phosphorylation in liver but not in inguinal adipose tissue suggesting that non-diabetic mice are less responsive to AT_2R activation than diabetic counterparts.

Overall, our findings demonstrate that activation of AT_2Rs through the administration of the selective AT_2R agonist C21 improved glucose and pyruvate tolerance in female db/db mice. These changes were associated with decreased liver weight, fibrosis, lipid deposition and TNF-α abundance as well as with improved insulin signaling in this tissue. Inguinal fat weight and adipocyte size were significantly reduced after C21 administration while both tissue and circulating levels of adiponectin were increased, indicative of improved insulin sensitivity. Further mechanistic analysis revealed that NO might mediate many of the C21 beneficial effects during diabetes. In conclusion, drugs targeting the AT_2R may represent a therapeutic option to prevent diabetes and alleviate its complications.

Accepted Article

This article is protected by copyright. All rights reserved.

REFERENCES

Alexander, S.P.H., Roberts, R.E., Broughton, B.R.S., Sobey, C.G., George, C.H., Stanford, SC, … Ahluwalia A,. (2018). Goals and practicalities of immunoblotting and immunohistochemistry: A guide for submission to the *British Journal of Pharmacology*. *British Journal of Pharmacology,* 175, 407–411. https://doi.org/10.1111/bph.14112

Alexander, S.P.H., Christopoulos, A., Davenport, A.P., et al. THE CONCISE GUIDE TO PHARMACOLOGY 2019/20: G protein-coupled receptors (2019). *British Journal of Pharmacology*, 176 Suppl 1(Suppl 1):S21-S141. https://doi:10.1111/bph.14748

Bataller, R., Sancho-Bru, P., Gines, P., Lora, J.M., Al-Garawi, A., Sole, M.,… Rodes, J. (2003). Activated human hepatic stellate cells express the renin-angiotensin system and synthesize angiotensin II. *Gastroenterology*, 125, 117–125. https://doi.org/10.1016/s0016-5085(03)00695-4

Berg, A.H., Combs, T.P., Du, X., Brownlee, M., & Scherer, P.E. (2001). The adipocyte-secreted protein Acrp30 enhances hepatic insulin action. *Nature Medicine,* 7, 947–953. https://doi.org/10.1038/90992

Carey, R.M. (2017). Update on angiotensin AT2 receptors. *Current Opinion in Nephrology and Hypertension,* 26, 91–96. https://doi.org/ 10.1097/MNH.0000000000000304

Curtis, M. J., Alexander, S., Cirino, G., Docherty, J. R., George, C. H., Giembycz, M. A., … Ahluwalia, A. (2018). Experimental design and analysis and their reporting II: Updated and simplified guidance for authors and peer reviewers. *British Journal of Pharmacology*, 175,987–993. https://doi.org/10.1111/bph.14153

Eriguchi, M., Bernstein, E.A., Veiras, L.C., Khan, Z., Cao, D.Y., Fuchs, S.,…Giani, J.F. (2018). The Absence of the ACE N-domain decreases renal inflammation and facilitates sodium excretion during diabetic kidney disease. *Journal of the American Society of Nephrology:JASN,* 29, 2546–2561. https://doi.org/ 10.1681/ASN.2018030323

Fang, X. & Sweeney, G. (2006). Mechanisms regulating energy metabolism by adiponectin in obesity and diabetes. *Biochemical Society Transactions,* 34, 798–801. https://doi.org/ 10.1042/BST0340798

Forrester, S.J., Booz, G.W., Sigmund, C.D., Coffman, T.M., Kawai, T., Rizzo, V.,…Eguchi, S. (2018). Angiotensin II signal transduction: an update on mechanisms of physiology and pathophysiology. *Physiological Reviews,* 98, 1627–1738. https://doi.org/ 10.1152/physrev.00038.2017

This article is protected by copyright. All rights reserved.

Harding, S.D., Sharman, J.L., Faccenda, E., Southan, C., Pawson AJ, Ireland S, Gray AJG, Bruce L, Alexander SPH, Anderton S, Bryant C, Davenport AP, Doerig C, Fabbro D, Levi-Schaffer F, Spedding M, Davies JA, NC-IUPHAR (2018). The IUPHAR/BPS Guide to PHARMACOLOGY in 2018: updates and expansion to encompass the new guide to IMMUNOPHARMACOLOGY. Nucleic Acids Res, 46, D1091-1106. https://doi:10.1093/nar/gkx1121.

Henriksen, E.J. (2007). Improvement of insulin sensitivity by antagonism of the renin-angiotensin system. *American Journal of Physiology. Regulatory, Integrative and Comparative Physiology,* 293, R974–R980. https://doi.org/ 10.1152/ajpregu.00147.2007

Hilliard, L.M., Chow, C.L., Mirabito, K.M., Steckelings, U.M., Unger, T., Widdop, R.E. & Denton KM. (2014). Angiotensin type 2 receptor stimulation increases renal function in female, but not male, spontaneously hypertensive rats. *Hypertension*, 64, 378–383. https://doi.org/ 10.1161/HYPERTENSIONAHA.113.02809

Hilliard, L.M., Jones, E.S., Steckelings, U.M., Unger, T., Widdop, R.E. & Denton, K.M. (2012). Sex-specific influence of angiotensin type 2 receptor stimulation on renal function: a novel therapeutic target for hypertension. *Hypertension*, 59**:** 409–414. https://doi.org/ 10.1161/HYPERTENSIONAHA.111.184986

Iimura, O., Shimamoto, K., Matsuda, K., Masuda, A., Takizawa, H., Higashiura, K.,…Nakagawa, M. (1995). Effects of angiotensin receptor antagonist and angiotensin converting enzyme inhibitor on insulin sensitivity in fructose-fed hypertensive rats and essential hypertensives. *American Journal of Hypertension,* 8, 353–357. https://doi.org/10.1016/0895-7061(94)00245-7

Kahn, S.E., Hull, R.L. & Utzschneider, K.M. (2006). Mechanisms linking obesity to insulin resistance and type 2 diabetes. *Nature,* 444, 840–846. https://doi.org/10.1038/nature05482

Kilkenny, C., Browne, W.J., Cuthill, I.C., Emerson, M. & Altman, D.G. (2010). Improving bioscience research reporting: the ARRIVE guidelines for reporting animal research. *PLoS Biology*, 8, e1000412. https://doi.org/ 10.1371/journal.pbio.1000412

Kubota, N., Terauchi, Y., Yamauchi, T., Kubota, T., Moroi, M., Matsui, J.,…Noda, T.. (2002). Disruption of adiponectin causes insulin resistance and neointimal formation. *The Journal of Biological Chemistry,* 277, 25863–25866. https://doi.org/ 10.1074/jbc.C200251200

Mauvais-Jarvis, F. (2015). Sex differences in metabolic homeostasis, diabetes, and obesity. *Biology of Sex Differences*, 6, 14. https://doi.org/ 10.1186/s13293-015-0033-y

McLaughlin, T., Craig, C., Liu, L.F., Perelman, D., Allister, C., Spielman, D. & Cushman, S.W. (2016). Adipose cell size and regional fat deposition as predictors of metabolic response to overfeeding in insulin-resistant and insulin-sensitive humans. *Diabetes*, 65, 1245–1254. https://doi.org/ 10.2337/db15-1213

This article is protected by copyright. All rights reserved.

Mehlem, A., Hagberg, C.E., Muhl, L., Eriksson, U. & Falkevall, A. (2013). Imaging of neutral lipids by oil red O for analyzing the metabolic status in health and disease. *Nature Protocols*, 8, 1149–1154. https://doi.org/ 10.1038/nprot.2013.055

Munoz, M.C., Giani, J.F., Dominici, F.P., Turyn, D. & Toblli, J.E. (2009). Long-term treatment with an angiotensin II receptor blocker decreases adipocyte size and improves insulin signaling in obese Zucker rats. *Journal of Hypertension,* 27, 2409–2420. https://doi.org/ 10.1097/HJH.0b013e3283310e1b

Nabeshima, Y., Tazuma, S., Kanno, K., Hyogo, H., Iwai, M., Horiuchi, M. & Chayama, K. (2006). Anti-fibrogenic function of angiotensin II type 2 receptor in CCl4-induced liver fibrosis. *Biochemical and Biophysical Research Communications*, 346, 658–664. https://doi.org/10.1016/j.bbrc.2006.05.183

Nag, S., Khan, M.A., Samuel, P., Ali, Q. & Hussain, T. (2015). Chronic angiotensin AT_2R activation prevents high-fat diet-induced adiposity and obesity in female mice independent of estrogen. *Metabolism*, 64, 814–825. https://doi.org/ 10.1016/j.metabol.2015.01.019

Nag, S., Patel, S., Mani, S. & Hussain, T. (2019). Role of angiotensin type 2 receptor in improving lipid metabolism and preventing adiposity. *Molecular and Cellular Biochemistry*, 461,195–204. https://doi.org/ 10.1007/s11010-019-03602-y

Ohshima, K., Mogi, M., Jing, F., Iwanami, J., Tsukuda, K., Min, L.J.,…Horiuchi, M. (2012). Direct angiotensin II type 2 receptor stimulation ameliorates insulin resistance in type 2 diabetes mice with PPARγ activation. *PloS One,* 7, e48387. https://doi.org/ 10.1371/journal.pone.0048387

Papatheodorou, K., Banach, M., Bekiari, E., Rizzo, M. & Edmonds, M. (2018). Complications of diabetes 2017. *Journal of Diabetes Research*, 2018, 3086167. https://doi.org/ 10.1155/2018/3086167

Paulis, L., Foulquier, S., Namsolleck, P., Recarti, C., Steckelings, U.M. & Unger, T. (2016). Combined angiotensin receptor modulation in the management of cardio-metabolic disorders. *Drugs,* 76, 1–12. https://doi.org/ 10.1007/s40265-015-0509-4

Peluso, A.A., Bertelsen, J.B., Andersen, K., Mortsensen, T.P., Hansen, P.B., Sumners, C.,… Steckelings U.M. (2018). Identification of protein phosphatase involvement in the AT2 receptor-induced activation of endothelial nitric oxide synthase. *Clinical Science*, 132, 777–790. https://doi.org/ 10.1042/CS20171598

Petersen, M.C. & Shulman, G.I. (2018). Mechanisms of insulin action and insulin resistance. *Physiological Reviews*, 98, 2133–2223. https://doi.org/ 10.1152/physrev.00063.2017

Quiroga, D.T., Munoz, M.C., Gil, C., Pffeifer, M., Toblli, J.E., Steckelings UM,…Dominici, F.P. (2018). Chronic administration of the angiotensin type 2 receptor agonist C21 improves insulin sensitivity in C57BL/6 mice. *Physiological Reports*, 6, e13824. https://doi.org/ 10.14814/phy2.13824

This article is protected by copyright. All rights reserved.

Ran, J., Hirano, T. & Adachi, M. (2004). Angiotensin II type 1 receptor blocker ameliorates overproduction and accumulation of triglyceride in the liver of Zucker fatty rats. *American Journal of Physiology. Endocrinology and Metabolism,* 287, E227–E232. https://doi.org/ 10.1152/ajpendo.00090.2004

Rodriguez, R., Minas, J.N., Vazquez-Medina, J.P., Nakano, D., Parkes, D.G., Nishiyama, A.,…Ortiz, R.M. (2018). Chronic AT1 blockade improves glucose homeostasis in obese OLETF rats. *The Journal of Endocrinology*, 237, 271–284. https://doi.org/ 10.1530/JOE-17-0678

Salans, L.B., Knittle, J.L. & Hirsch, J. (1968). The role of adipose cell size and adipose tissue insulin sensitivity in the carbohydrate intolerance of human obesity. *The Journal of Clinical Investigation*, 47, 153–165. https://doi.org/ 10.1172/JCI105705

Sansbury, B.E. & Hill. B.G. (2014). Regulation of obesity and insulin resistance by nitric oxide. *Free Radical Biology & Medicine,* 73, 383–399. https://doi.org/ 10.1016/j.freeradbiomed.2014.05.016

Santos, R.A.S., Oudit, G.Y., Verano-Braga, T., Canta, G., Steckelings, U.M. & Bader, M. (2019). The renin-angiotensin system: going beyond the classical paradigms. *American Journal of Physiology. Heart and Circulatory Physiology*, 316, H958–H970. https://doi.org/ 10.1152/ajpheart.00723.2018

Schmidt, S.A.J., Lo, S. & Hollestein, L.M. (2018). Research techniques made simple: sample size estimation and power calculation. *The Journal of Investigative Dermatology*, 138, 1678–1682. https://doi.org/ 10.1016/j.jid.2018.06.165

Shao, C., Yu, L. & Gao, L. (2014). Activation of angiotensin type 2 receptors partially ameliorates streptozotocin-induced diabetes in male rats by islet protection. *Endocrinology,* 155,793–804. https://doi.org/ 10.1210/en.2013-1601

Shao, C., Zucker, I.H. & Gao, L. (2013). Angiotensin type 2 receptor in pancreatic islets of adult rats: a novel insulinotropic mediator. *American Journal of Physiology. Endocrinology and Metabolism*, 305, E1281–E1291. https://doi.org/ 10.1152/ajpendo.00286.2013

Shiuchi, T., Iwai, M., Li, H.S., Wu, L., Min, L.J., Li, J.M.,…Horiuchi, M. (2004). Angiotensin II type-1 receptor blocker valsartan enhances insulin sensitivity in skeletal muscles of diabetic mice. *Hypertension*, 43, 1003–1010. https://doi.org/ 10.1161/01.HYP.0000125142.41703.64

Shoelson, S.E., Lee, J., & Goldfine, A.B. (2006). Inflammation and insulin resistance. *The Journal of Clinical Investigation*, 116, 1793–1801. https://doi.org/10.1172/JCI29069

Shum, M., Pinard, S., Guimond, M.O., Labbe, S.M., Roberge, C., Baillargeon, J.P.,…Gallo-Payet, N. (2013). Angiotensin II type 2 receptor promotes adipocyte differentiation and restores adipocyte size in high-fat/high-fructose diet-induced insulin resistance in rats. *American Journal of Physiology. Endocrinology and Metabolism,* 304, E197–E210. https://doi.org/10.1152/ajpendo.00149.2012

This article is protected by copyright. All rights reserved.

Silva-Antonialli, M.M., Tostes, R.C., Fernandes, L., Fior-Chadi, D.R., Akamine, E.H., Carvalho, M.H.,…Nigro, D. (2004). A lower ratio of AT1/AT2 receptors of angiotensin II is found in female than in male spontaneously hypertensive rats. *Cardiovascular Research*, 62, 587–593. https://doi.org/ 10.1016/j.cardiores.2004.01.02

Siragy, H.M. & Carey, R.M. (1997). The subtype 2 (AT2) angiotensin receptor mediates renal production of nitric oxide in conscious rats. *The Journal of Clinical Investigation*, 100, 264–269. https://doi.org/ 10.1172/JCI119531

Steckelings, U.M., Kaschina, E. & Unger, T. (2005). The AT2 receptor--a matter of love and hate. *Peptides*, 26, 1401–1409. https://doi.org/ 10.1016/j.peptides.2005.03.010

Steckelings, U.M., Larhed, M., Hallberg, A., Widdop, R.E., Jones, E.S., Wallinder, C.,...Unger, T. (2011). Non-peptide AT2-receptor agonists. *Current Opinion in Pharmacology*, 11**,** 187–192. https://doi.org/10.1016/j.coph.2010.11.002

Takata, H., Yamada, H., Kawahito, H., Kishida, S., Irie, D., Kato, T.,…Matsubara, H. (2015). Vascular angiotensin II type 2 receptor attenuates atherosclerosis via a kinin/NO-dependent mechanism. *Journal of the Renin-Angiotensin-Aldosterone System*, 16, 311–320. https://doi.org/ 10.1177/1470320313491794

Than, A., Xu, S., Li, R., Leow, M.K., Sun, L. & Chen, P. (2017). Angiotensin type 2 receptor activation promotes browning of white adipose tissue and brown adipogenesis. *Signal Transduction and Targeted Therapy*, 2, 17022. https://doi.org/10.1038/sigtrans.2017.22

Tilg, H. & Moschen, A.R. (2010). Evolution of inflammation in nonalcoholic fatty liver disease: the multiple parallel hits hypothesis. *Hepatology*, 52, 1836–1846. https://doi.org/ 10.1002/hep.24001

Toblli, J.E., Munoz, M.C., Cao, G., Mella, J., Pereyra, L. & Mastai, R. (2008). ACE inhibition and AT1 receptor blockade prevent fatty liver and fibrosis in obese Zucker rats. *Obesity*, 16, 770–776. https://doi.org/ 10.1038/oby.2007.114

Umanath, K. & Lewis, J.B. (2018). Update on diabetic nephropathy: core curriculum 2018. *American journal of kidney diseases: the official journal of the National Kidney Foundation,* 71, 884–895. https://doi.org/ 10.1053/j.ajkd.2017.10.026

Wang, L., Wang, Y., Li, X.Y. & Leung, P.S. (2017). Angiotensin II type 2 receptor activation with compound 21 augments islet function and regeneration in streptozotocin-induced neonatal rats and human pancreatic progenitor cells. *Pancreas*, 46, 395–404. https://doi.org/ 10.1097/MPA.0000000000000754

Warner, F.J., Lubel, J.S., McCaughan, G.W. & Angus, P.W. (2007). Liver fibrosis: a balance of ACEs? *Clinical Science*, 113, 109–118. https://doi.org/ 10.1042/CS20070026

This article is protected by copyright. All rights reserved.

Yan, F., Yuan, Z., Wang, N., Carey, R.M., Aylor, K.W., Chen, L.,…Liu, Z. (2018). Direct activation of angiotensin II type 2 receptors enhances muscle microvascular perfusion, oxygenation, and insulin delivery in male rats. *Endocrinology* 159, 685–695. https://doi.org/ 10.1210/en.2017-00585

Yang, Y.M. & Seki, E. (2015). TNFα in liver fibrosis. *Current Pathobiology Reports,* 3**,** 253–261. https://doi.org/ 10.1007/s40139-015-0093-z

Accepted Article

This article is protected by copyright. All rights reserved.

Table 1 - Female diabetic (db/db) and their respective control (db/+) mice received a subcutaneous treatment with either saline or C21 for 4 weeks. A subgroup of C21-treated mice also received L-NAME in the drinking water. Tissue weight for heart, liver and inguinal and perirenal adipose tissue were measured at the end of the experiment. Data are expressed as mean ± SD. **P*<0.05 vs. the corresponding db/+ group. $^{\#}$*P*<0.05 vs. db/db saline group. †*P*<0.05 vs. db/db C21 + L-NAME group.

	db/+ Saline	**db/db Saline**	**db/+ C21**	**db/db C21**	**db/+ C21+L-NAME**	**db/db C21+L-NAME**
Heart (g)	0.14 ± 0.02	0.17 ± 0.03	0.15 ± 0.02	0.17 ± 0.02	0.14 ± 0.02	0.16 ± 0.02
Inguinal fat (g)	0.4 ± 0.1	1.8 ± 0.5*	0.4 ± 0.1	1.2 ± 0.5*$^{\#\dagger}$	0.34 ± 0.06	1.7 ± 0.2*
Perirenal fat (g)	0.5 ± 0.2	2.6 ± 0.6*	0.6 ± 0.1	1.8 ± 0.4*$^{\#\dagger}$	0.5 ± 0.1	2.8 ± 0.6*
Liver (g)	0.9 ± 0.1	3.7 ± 0.7*	0.9 ± 0.2	2.7 ± 0.8*$^{\#}$	0.9 ± 0.1	3.2 ± 0.5*

This article is protected by copyright. All rights reserved.

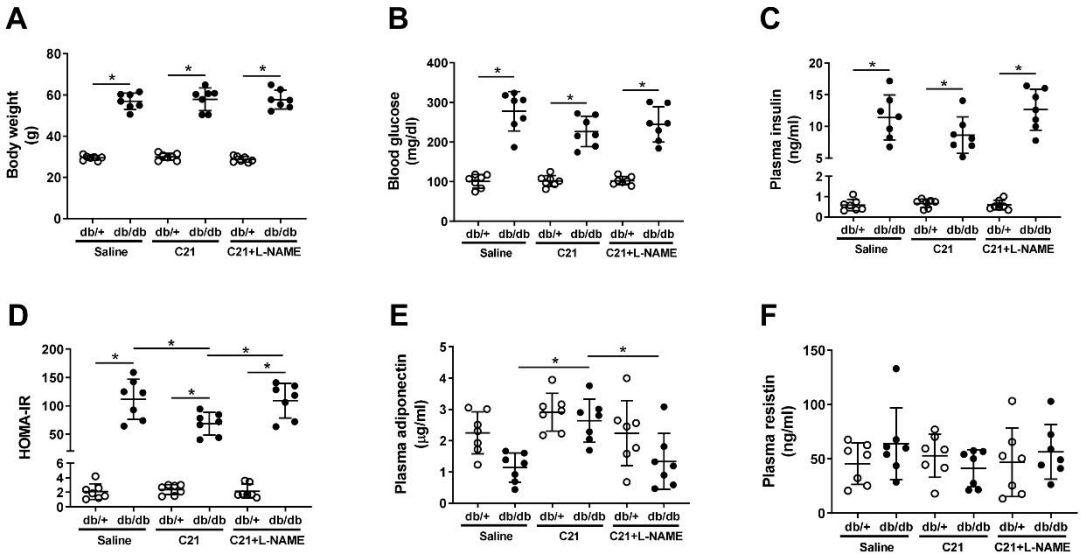

Figure 1 - Chronic C21 treatment improves insulin sensitivity and increases plasma levels of adiponectin in diabetic mice. Body weight (A), blood glucose (B), plasma insulin (C), HOMA-IR (D), plasma adiponectin (E) and plasma resistin (F) were assessed at the end of the experiment. Data are expressed as mean ± SD. **P*<0.05 (n = 7 per group).

This article is protected by copyright. All rights reserved.

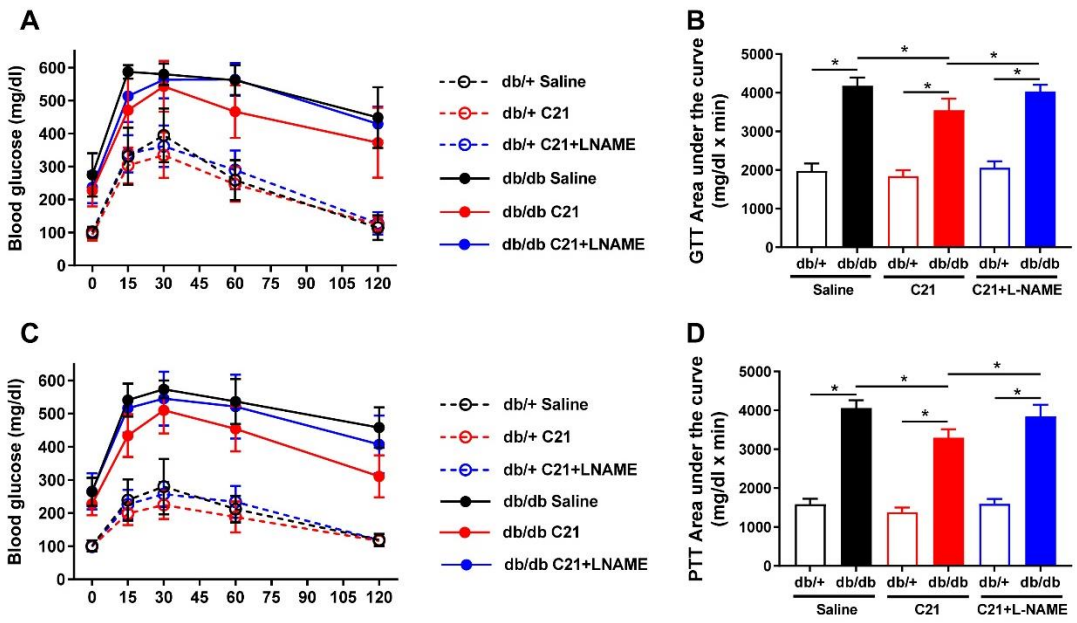

Figure 2 - Chronic administration of C21 improves glucose and pyruvate tolerance in female db/db mice. Glucose tolerance test (A) and pyruvate tolerance test (C) were performed as described in Methods. For this, basal glucose was measured after a 6-hour fast and reanalyzed at 15, 30, 60, and 120 min post-injection of either glucose or pyruvate. The area under the curve was calculated for each experimental group (B and D). Data are expressed as mean ± SD. *P<0.05 (n = 7 per group). GTT: Glucose tolerance test. PTT: Pyruvate tolerance test.

Accepted

This article is protected by copyright. All rights reserved.

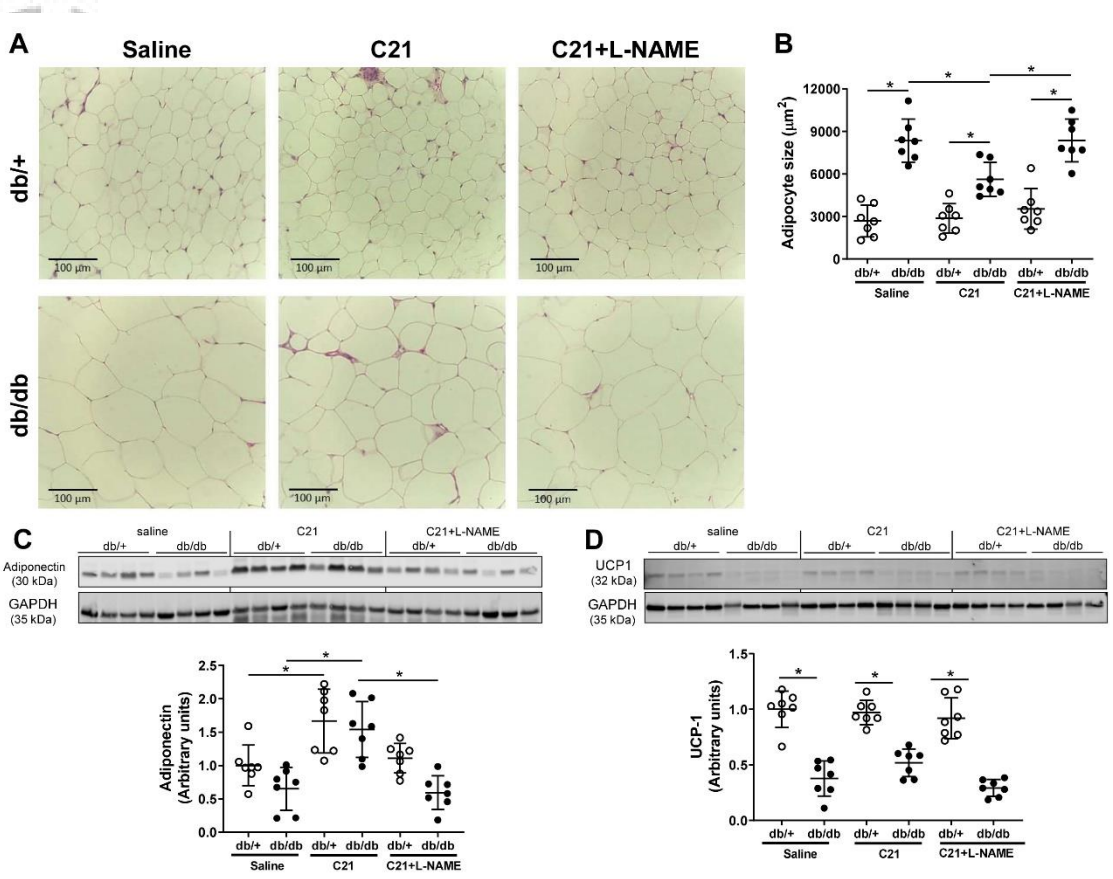

Figure 3 - C21 decreases adipocyte cell size and increases adiponectin levels in inguinal adipose tissue. These effects are prevented with L-NAME. Paraffin sections (3 µm) of inguinal adipose tissue were stained with hematoxylin and eosin and images acquired as described in Methods. Representative histology images were obtained in adipose tissue sections at x20 magnification (A). To evaluate the adipocyte size distribution, the average area of 60 adipocytes was measured in five different microscopic fields for each sample (B). Adiponectin (C) and UCP1 (D) were measured in homogenates of inguinal adipose tissue by Western blot. Glyceraldehyde 3-phosphate dehydrogenase (GAPDH) confirms equal protein amount in each sample. Data are expressed as mean ± SD. **P*<0.05 (n = 7 for all groups).

This article is protected by copyright. All rights reserved.

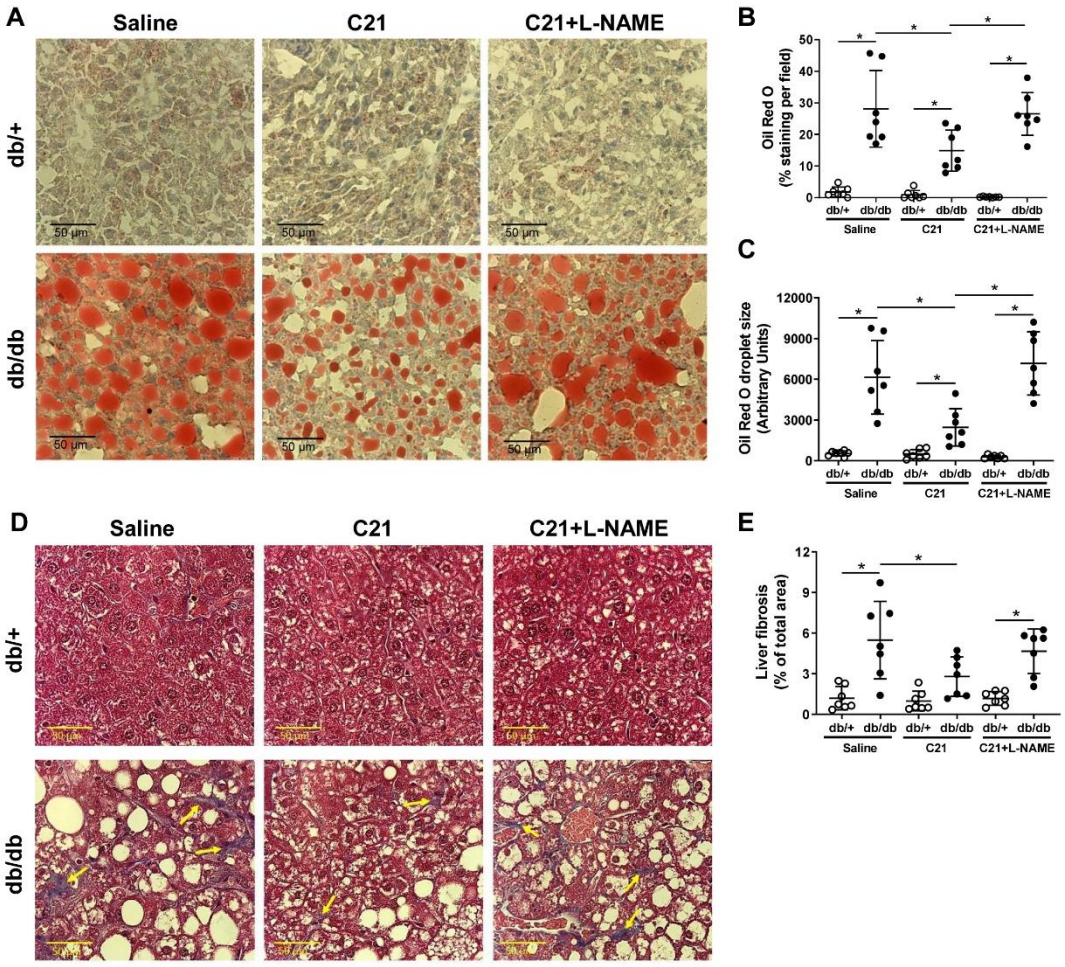

Figure 4 - Chronic C21 administration decreases lipid accumulation in the liver of db/db mice. These effects were partially blunted with L-NAME. Frozen liver sections (8 µm) were stained with oil red O as described in Methods (A). The area of positive staining per field (B) and the average size of lipid droplets (C) were calculated using ImageJ. For fibrosis assessment, paraffin sections (3 µm) of liver tissue were stained with Masson's trichrome staining (D). Percentage of fibrosis (indicated with yellow arrows) per total area (E) was calculated using ImageJ. Analysis was performed in 10 representative histology images obtained at x20 magnification. Bars represent 50 µm. Data are expressed as mean ± SD. **P*<0.05 (n = 7 for all groups).

This article is protected by copyright. All rights reserved.

Accepted Article

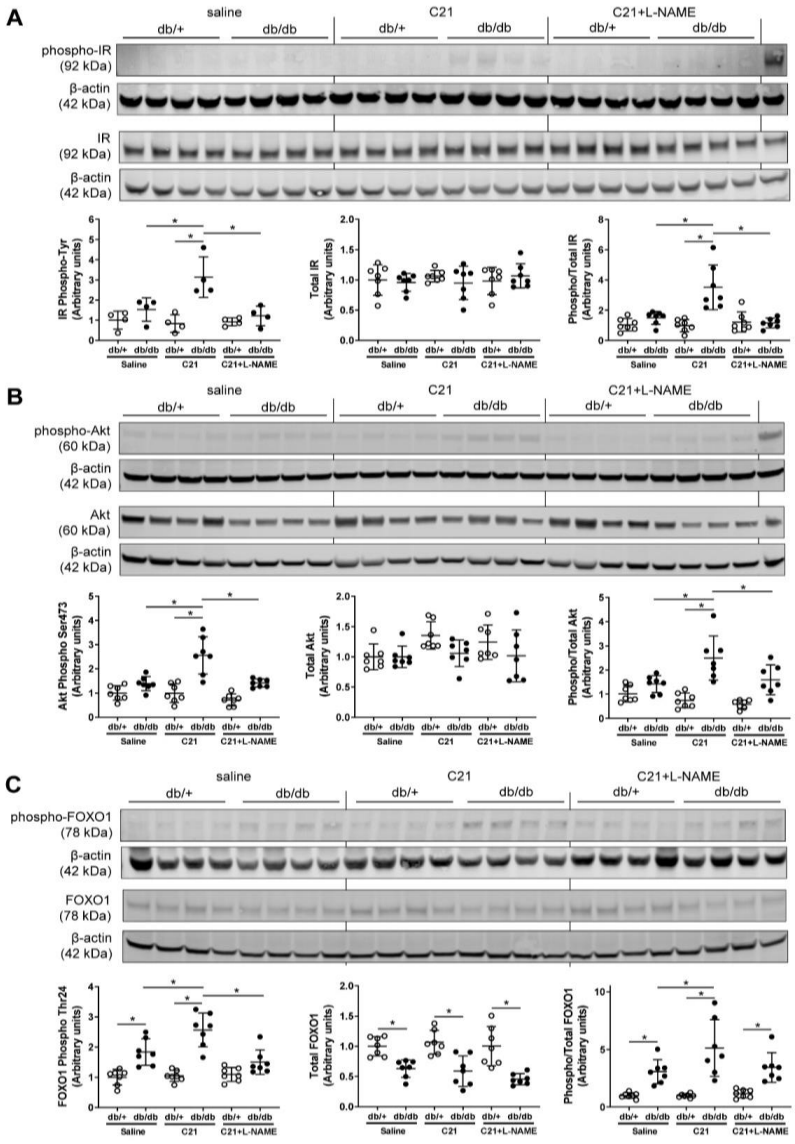

Figure 5 - C21 increases the phosphorylation of insulin signaling molecules in liver of db/db mice. The phosphorylation level and total abundance of the insulin receptor (IR), Akt (B) and FOXO1 (C) were evaluated in liver homogenates by Western blot. Western blot membranes were re-probed with an anti-β-actin antibody for loading control and each sample was corrected by its corresponding β-actin value. The phosphorylation-to-protein ratio was calculated for each sample. Positive controls for IR and Akt (rightmost bands) are liver homogenates from db/+ mice injected with 5 µg of insulin. Data are expressed as mean ± SD. **P*<0.05 (n = 7 for all groups).

This article is protected by copyright. All rights reserved.

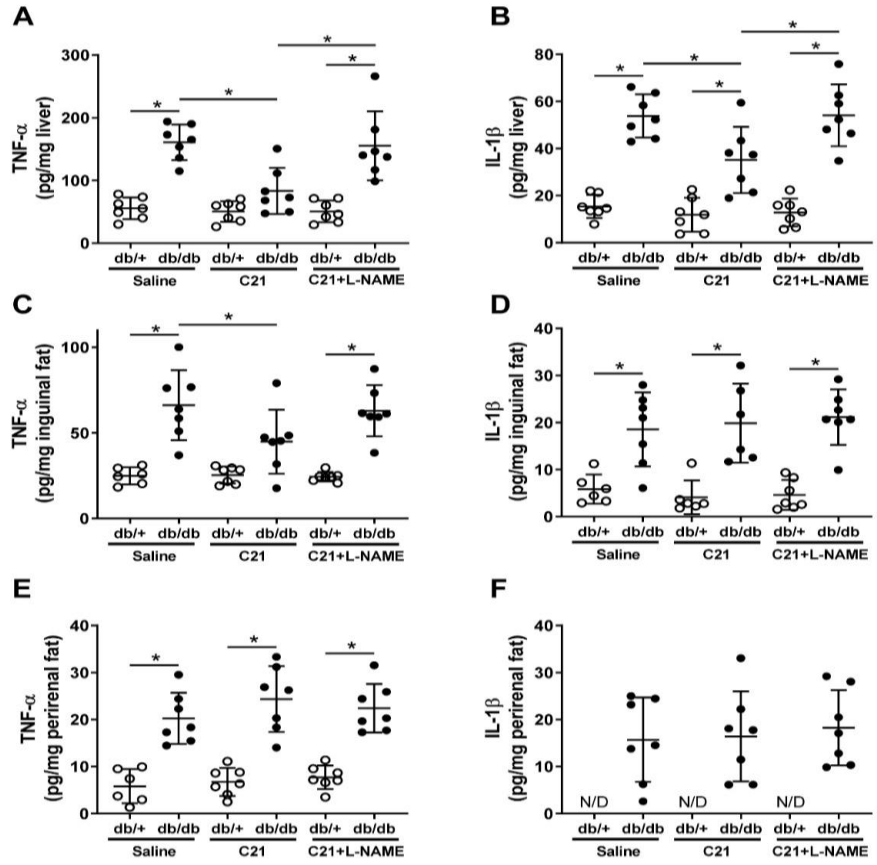

Figure 6 - Diabetic db/db mice treated with C21 display lower levels of pro-inflammatory cytokines in the liver. TNFα (A) and interleukin (IL)-1β (B) were measured in total liver (A,B; n = 7 for all groups) and inguinal (C,D; n = 6 for db/+ Saline and n = 7 for all other groups) and perirenal (E,F; n = 6 for db/+ Saline and n = 7 for all other groups) adipose tissue homogenates using a commercial ELISA as described in Methods section. Data are expressed as mean ± SD. *P<0.05.

This article is protected by copyright. All rights reserved.

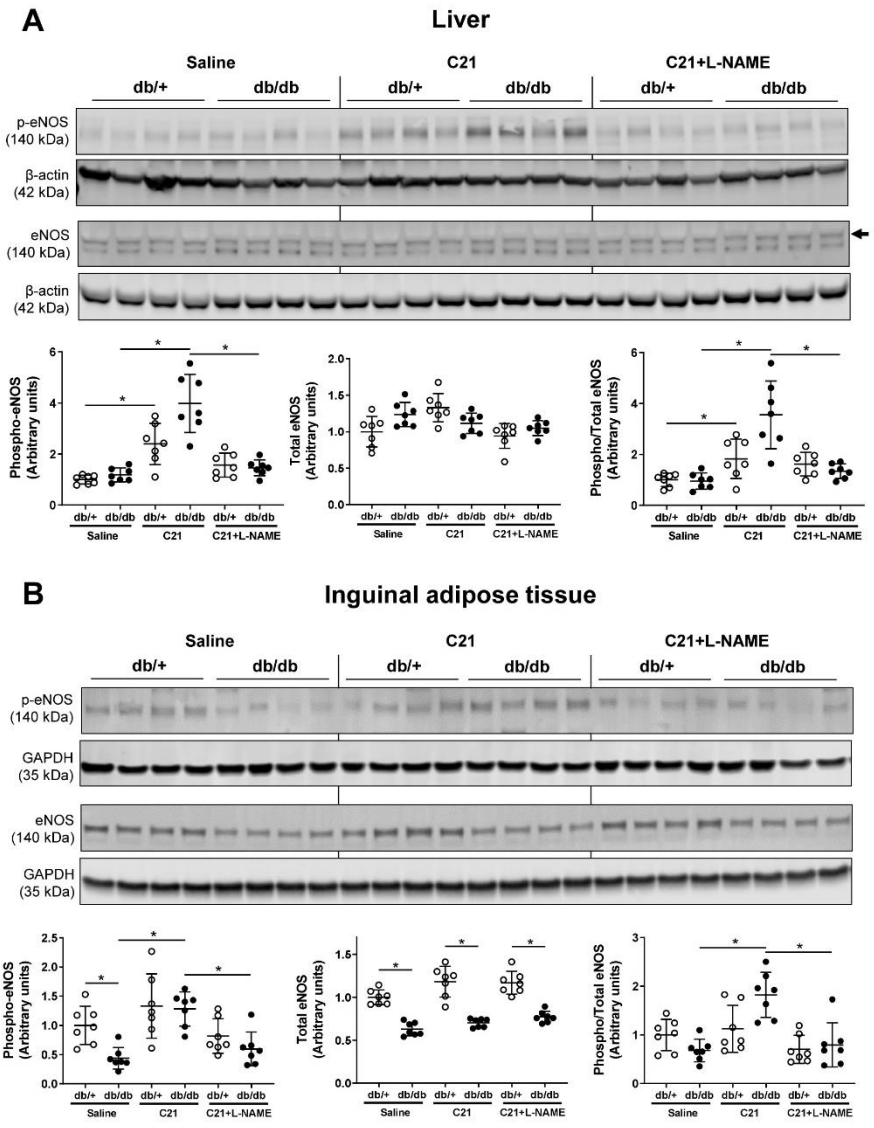

Figure 7 - C21 increased the phosphorylation at Ser1177 of endothelial nitric oxide synthase (eNOS) in liver and inguinal adipose tissue of female db/db mice that was prevented with a chronic administration of a sub-pressor dose of L-NAME (0.1 mg ml^{-1} in the drinking water). The phosphorylation at Ser1177 and the total abundance of eNOS were evaluated in liver (A) and inguinal fat (B) homogenates by Western blot. Western blot membranes were re-probed with an anti-β-actin (liver) or anti-GAPDH (inguinal fat) antibody for loading control and each sample was corrected by its corresponding β-actin or GAPDH value. The phosphorylation-to-protein ratio was calculated for each sample. Data are expressed as mean ± SD. **P*<0.05 (n = 7 for all groups).

This article is protected by copyright. All rights reserved.